Draft version February 5, 2008
Preprint typeset using LaTeX style emulateapj v. 11/26/04

arXiv:astro-ph/0508555v1 25 Aug 2005

CONSTRAINING THE DISTRIBUTION OF L- & T-DWARFS IN THE GALAXY*

R. E. Ryan Jr., N. P. Hathi, S. H. Cohen & R. A. Windhorst[2]
Department of Physics and Astronomy, Arizona State University, Tempe, AZ 85281

Draft version February 5, 2008

ABSTRACT

We estimate the thin disk scale height of the Galactic population of L- & T-dwarfs based on star counts from 15 deep parallel fields from the Hubble Space Telescope. From these observations, we have identified 28 candidate L- & T-dwarfs based on their $(i'-z')$ color and morphology. By comparing these star counts to a simple Galactic model, we estimate the scale height to be 350 ± 50 pc that is consistent with the increase in vertical scale with decreasing stellar mass and is independent of reddening, color-magnitude limits, and other Galactic parameters. With this refined measure, we predict that less than 10^9 $M_\odot$ of the Milky Way can be in the form L- & T-dwarfs, and confirm that high-latitude, $z\simeq6$ galaxy surveys which use the i'-band dropout technique are 97-100% free of L- & T-dwarf interlopers.

Subject headings: stars: low-mass, brown dwarfs — Galaxy: structure — Galaxy: stellar content

1. INTRODUCTION

The method of counting stars to infer the shape and size of the Galaxy is as old as astronomy itself. Earliest efforts using this technique were famously flawed as they often relied on insufficient data or wholly incorrect assumptions (eg. Herschel 1785; Kapteyn 1922). Aided by advanced technology, Bahcall & Soneira (B&S; 1980, 1981) demonstrated that the true power of star counts is realized when they are compared to simulations of the fundamental equation of stellar statistics (von Seeliger 1898). The B&S method relies heavily on the assumed luminosity functions and density distributions, and has been a standard method for many subsequent studies.

The Galaxy is traditionally characterized by having a Population I disk and Population II spheroid. In a series of studies of the exponential disk, Gilmore & Reid (1983) and Gilmore (1984) established the need for a thick and thin disk whose scale heights are inversely proportional to the masses of the studied stars (see Table 1 in Siegel et al. 2002). The standard description of the Galactic halo is a de Vaucouleur or power-law profile, while the Besançon flattened spheroid with $c/a\approx0.5-0.8$ (Bahcall & Soneira 1984; Robin, Reylé, & Crézé 2000; Larsen & Humphreys 2003; Robin et al. 2003) being the currently favored parameters. Thorough discussions of star counts and their relevance to Galactic structure are given in the Annual Reviews by Bahcall (1986), Gilmore, Wyse, & Kuijken (1989), and Majewski (1993).

Many of the Galactic models and the majority of the literature examine on relatively luminous dwarf and/or giant stars and rarely address sub-stellar objects. The discovery of the first extra-solar, sub-stellar object, Gliese 229B (Nakajima et al. 1995; Oppenheimer et al. 1995) motivated the creation of the L and T spectral classes. With surface temperatures ranging from 750–2200 K (Burgasser 1999), the L- & T-dwarfs can contaminate searches for $z\simeq6$, i'-band dropout objects (Yan, Windhorst, & Cohen 2003) by mimicking the extremely red broad-band colors. This effect has remained largely unquantified due to insufficient knowledge of the L- & T-dwarf IMF, Galactic distribution, and local number density. Previous work on their IMF and local number density (Reid et al. 1999; Chabrier 2001, 2002; Liu et al. 2002) has suffered from limited statistics. With the deep imaging of 15 Hubble Space Telescope (HST) Advanced Camera for Surveys (ACS) parallel fields, this study increases the number of *faint* dwarfs by adding 28 to the growing list. Little work has been done on the scale height of L- & T-dwarfs; Liu et al. (2002) and Pirzkal et al. (2005) estimated 100–400 pc as based on a single object or a 3–4 objects in a single field. Therefore the primary goal of this work is to estimate the scale height of the L- & T-dwarf population by comparing the surface densities from the ACS parallel fields to the Galactic structure models.

2. OBSERVATIONS

The L- & T-dwarf candidates were selected from 15 HST/ACS parallel fields covering a broad range in Galactic latitudes and longitudes (see Table 1). All ACS fields have at least three independent exposures in F775W (SDSS-i') and F850LP (SDSS-z') with a total exposure time of 2–10 ks per bandpass. All fields are ≥90% complete at z'(AB)≃26.0 mag (Yan & Windhorst 2004a). We adopt the AB magnitude system (Oke & Gunn 1983).

After combining the individual ACS frames into final stacks using the PyRAF-based script *multidrizzle* (Koekemoer et al. 2002), the SExtractor package (Bertin & Arnouts 1996) was used in double-input mode to perform the matched-aperture photometry. The F850LP stack was used to define the optimal apertures for the flux measurements in both stacks. For source detection, we used a 5×5 Gaussian smoothing kernel with a FWHM of 2.0 pixels, which is approximately the same as the FWHM of the ACS point-spread function (PSF) on both image stacks. We used total magnitudes (corre-

---

*Based on observations made with the NASA/ESA Hubble Space Telescope, obtained from the data archive at the Space Telescope Science Institute, which is operated by the Association of Universities for Research in Astronomy, Inc., under NASA contract NAS 5-26555.

Electronic address: Russell.Ryanjr@asu.edu

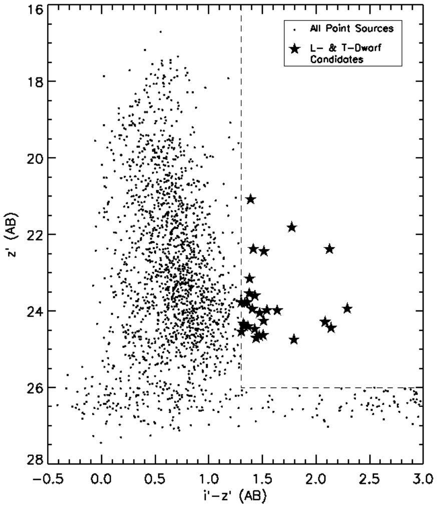

FIG. 1.— Color-magnitude diagram for all point sources detected in our 15 ACS fields. The small dots represent all objects that met the stellar morphology classification, the solid stars are the 28 L- & T-dwarf candidates, and the dashed lines represent the imposed color-magnitude limits. Many point sources associated with diffraction spikes, field edges, and spurious detections (objects smaller than the PSF, likely residual cosmic rays) brighter than $z' = 26$ mag were manually removed. The similar points fainter than $z' = 26$ mag were not removed from this figure. The sample of stellar candidates, becomes incomplete for $z' \geq 25$ mag.

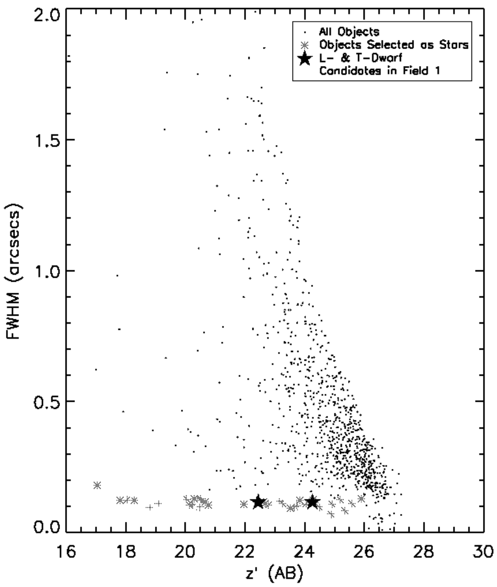

FIG. 2.— The observed FWHM for all objects in Field 1 is plotted as a function of apparent z' magnitude. The small dots, asterisks, and filled stars represent all objects, the point sources used to define the "stellar-locus," and the objects selected as candidate L- & T-dwarfs. Clearly many objects were recognized as point sources, however only two met the $(i'-z')$ color criterion.

TABLE 1
L- & T-DWARF NUMBER COUNTS

Field No.	$l^{\rm II}$ (deg)	$b^{\rm II}$ (deg)	Number (per 9 arcmin^2)
1	115.018	+46.681	2
2	164.056	−75.750	1
3	169.188	−59.664	0
4	279.934	−19.990	3
5	165.876	+36.396	0
6	280.782	+68.293	0
7	113.107	+28.548	2
8	293.996	−41.466	0
9	316.829	−40.490	1
10	105.103	+7.075	11
11	298.138	−13.885	6
12	92.666	+46.378	1
13	70.106	+62.876	0
14	251.327	−41.444	0
15	216.142	+54.561	1

sponding to the *MAG_AUTO* option in SExtractor) for the photometry and adopted the zero points published in HST ACS Instrument Science Report (De Marchi et al. 2004).

As a cursory selection, all objects with $(i'-z')>1.3$ mag and $z' < 26.0$ mag were considered. Figure 1 is the color-magnitude diagram for all point sources detected in all 15 fields. Dashed lines indicate the imposed color-magnitude limits and the large, filled stars represent the candidate L- & T-dwarfs. For the five fields for which the F475W (SDSS-g') band was available, we required candidates to have $(g'-i')>0$ mag. Objects near the detector edges were not considered, yielding an effective area of $\sim$9 arcmin^2 per ACS field. Extended objects were eliminated from the analysis by using the FWHM parameter of SExtractor. In Figure 2, we plot the FWHM as a function of apparent magnitude for each object in Field 1 as small dots. The locus of points at FWHM$\sim 0.''13$ and $z' < 26$ mag (hereafter the "stellar locus"), represented as asterisks, are the unresolved objects with the minimum possible FWHM. In addition to the above color-magnitude criterion, we required all L- & T-dwarf candidates to lie within this locus. Sources of contamination to these criteria are discussed in § 4.1.

Typically Galactic structure studies examine star counts from one or many shallow fields with large surveyed areas (eg. Siegel et al. 2002; Larsen & Humphreys 2003). Thus the data of the 2MASS (Burgasser 1999; Kirkpatrick et al. 1999), DENIS (Delfosse 1999), and/or SDSS (Strauss et al. 1999; Tsvetanov et al. 2000; Hawley et al. 2002) are natural choices to study the Galactic distribution of the L- & T-dwarfs. These surveys have significantly more detection area than our HST dataset and their L- & T-dwarfs are typically closer to the Sun than $\sim$300 pc or 1 disk scale height. Therefore to avoid *extrapolating* the vertical scale height beyond this distance, we chiefly analyzed the HST dataset where all sample stars are likely more distant than 1 e-folding length.

3. THE SIMPLE GALACTIC MODEL

The Galactic structure models were made by distributing 10^{10} points according to an exponential disk that was motivated by the light profiles of edge-on galaxies (de Grijs, Peletier, & van der Kruit 1996): $n(r,\theta,z) = n_0 \exp\left(\frac{R_0-r}{r_l}\right)\exp\left(\frac{Z_0-z}{z_h}\right)$, where r_l=2100 pc is the radial scale length found by Porcel et al (1998), n_0=0.12 pc^{-3} is the local space density L- & T-dwarfs taken from Chabrier (2002), and R_0=8 kpc and Z_0=15 pc (Yamagata & Yoshii 1992) are the solar ra-

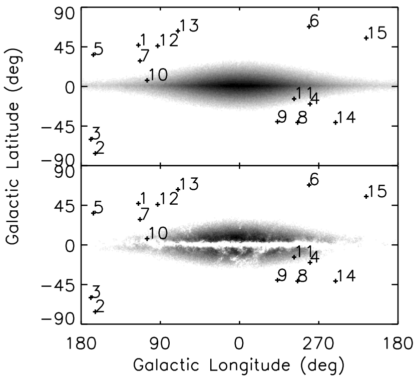

FIG. 3.— A sample realization of the Monte Carlo simulation with 10^{10} random points with the best-fit vertical scale height of 350 pc. The over-plotted crosses with numbers represent each of the observed HST/ACS field in Table 1. The effects of the Schlegel et al. (1998) dust maps are readily apparent when comparing the upper (no extinction) and lower (extinction) panels.

dius and height, respectively. The vertical scale height, z_h, is the free parameter and found by minimizing the squared difference between the number counts from the model and the HST data. Altering the assumed coordinates of the Sun and the radial scale length have little effect on the vertical scale height estimate. To generate absolute magnitudes, we adopted the J-band luminosity function of Cruz et al. (2003) and the $(z' - J)$ colors of Hawley et al. (2002) over the appropriate range of spectral type.

The effects of interstellar extinction were included into the model using the COBE dust maps of Schlegel et al. (1998) in two ways. First, we assumed that each point was located beyond the dust, establishing a lower bound on the model counts. Alternatively, an upper bound is reached by assuming that the Galaxy has *no* dust whatsoever. Since an overwhelming majority of the dust is localized to $|b^{\mathrm{II}}|\lesssim 15°$ (see Figure 3) and only two of our observed ACS fields are in this range, either approach yielded the same result within the uncertainties, therefore we adopted the third method for simplicity. Figure 3 is a representative realization the model with a scale height of 350 pc, the with locations of the 15 observed fields are indicated with plus signs.

The canonical disk/spheroid Galaxy likely has additional components (Bahcall 1986), the models used here did not contain any contribution from the Galactic bulge or a two-component disk (Gilmore & Reid 1983; Gilmore 1984) for the following reasons. First, a bulge distribution was not modeled since its radius is ∼1–2 kpc or ∼7°–14°, and every field is well beyond 14° of the Galactic center, hence we do not require a bulge component in the model. Second, this sample contains only 28 L- & T-dwarfs which are likely within ∼1000 pc (based on the luminosity function) of the Sun. Since the thick disk has a scale height of $\gtrsim$1000 pc, we expect the star counts to be dominated by a *single* disk population. Moreover, With only 28 candidates the models and analyses must remain simple and straightforward.

4. ANALYSIS

Despite this work utilizing the largest dataset of L- & T-dwarfs compiled from HST observations, the star counts remain very sparse requiring a simple analysis scheme. Using the grid of Monte Carlo models described in § 3, we sought the scale height which minimizes the squared difference between the integrated star counts of the model and those from the HST/ACS dataset. For the fields where no L- & T-dwarf candidates were found, we assumed an upper limit of one object (per field) could have been detected and perform this minimization technique simultaneously on all 15 fields. This procedure yielded a vertical scale height of 350±50 pc. In the upper panel of Figure 4, we plot the modeled surface density averaged over Galactic longitude as a function of Galactic latitude as computed from the model with a scale height of 350 pc, with the HST data points from Table 1 overplotted for comparison. The residuals in the lower panel clearly demonstrate that the model with a scale height of 350 pc reproduces the HST star counts for $|b^{\mathrm{II}}|\geq 15°$ where dust extinction is minimal.

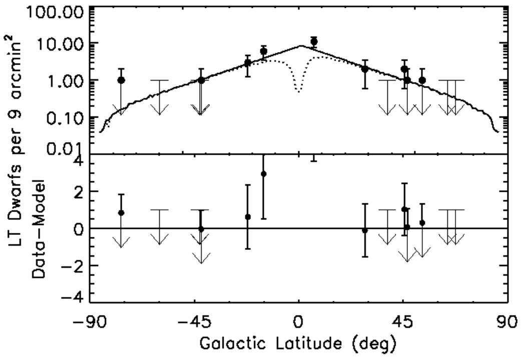

FIG. 4.— **Top panel:** model surface density as a function of Galactic latitude. Here we have averaged over all longitudes with a 2.5σ-clipping to better handle the sparse statistics at high latitudes. The dotted and full lines indicate models with and without the extinction corrections, respectively. The data from the 15 ACS fields are plotted for comparison as filled circles and downward arrows as an upper limit when either zero or one object was detected. **Bottom panel:** the residuals from the upper panel as a function of Galactic latitude. Clearly the data where the dust corrections are large (ie. $|b^{\mathrm{II}}|\lesssim 15°$) are the most deviant. The model used in both panels has a vertical scale height of 350 pc. The two fields outlying fields at $|b^{\mathrm{II}}|\lesssim 15°$ are discussed in § 4.1.

4.1. *Sources of Contamination*

While all L- & T-dwarf candidates were systematically found by color and FWHM criteria, each was visually confirmed as a point source. However, the color-magnitude rules outlined in § 2 potentially find three classes of contaminates:

(1) The primary motivation of this study is to reliably correct the $z \simeq 6$, i'-band dropout galaxy surveys for interloping L- & T-dwarfs (Yan et al. 2002; Yan, Windhorst, & Cohen 2003; Yan & Windhorst 2004a,b). Since our method is similar to the i'-band dropout technique, we expect possible contamination to the star counts from the $z \simeq 6$ galaxies. In a recent study of the Hubble Ultra-Deep Field (HUDF), Yan & Windhorst (2004b) find 108 i'-band dropouts using the $(i' - z')$>1.3 mag color selection. Their sample has a median z'-band magnitude of 28.5 mag, and contains only three objects brighter than our limit of z'=26.0 mag. Each of these three objects is considerably extended and could not be mistaken for a point-source. Since the majority of unresolved $z \simeq 6$ galaxies will be

∼2.5 mag too faint, we conclude their contamination in our sample must be negligible.

(2) Another known source of possible contaminates comes from dusty, elliptical galaxies with redshifts $1.0 \leq z \leq 1.5$, whose 4000 Å break occurs between the i' and z' bands (Yan, Windhorst, & Cohen 2003). With a typical color of $(i'-z')\sim 1.0$ mag, many of these objects would appear too blue in the absence of extreme internal reddening. Moreover the visual identification confirms only point-like objects populate the "stellar locus" in the lower left of Figure 2. Hence, extended elliptical galaxies could not grossly corrupt our sample.

(3) In addition to the above extragalactic sources, we anticipated contamination from galactic M-dwarfs for two different reasons. First, the color criterion of $(i'–z')>$ 1.3 mag was primarily motivated by the $z\simeq 6$ galaxy surveys and is ∼0.5 mag too blue (Hawley et al. 2002) to have included only L- & T-dwarfs. When we repeated the above analysis for $(i'-z')\geq 1.8$ mag (Hawley et al. 2002) the star counts were reduced by ∼50% and the inferred vertical scale height was 300 ± 100 pc. While there is a significant contribution from late M-dwarfs, the vertical scale height was unaffected by the 0.5 mag color difference. Second, an appreciably reddened M-dwarf could have an $(i'-z')$ color of an unreddened L- or T-dwarf. This scenario requires considerable reddening, only the two fields with $|b^{\rm II}|\lesssim 15^{\circ}$ have $E(i'-z')\gtrsim 0.1$ mag. This effect could account these fields lying more than 1σ above the best-fit line in Figure 4, however we cannot be certain without more broad-band filters or spectroscopy. We investigated this effect's contribution by removing the two suspect fields and repeated the analysis. While this procedure reduced the observed star counts by ∼50%, it resulted in a vertical scale height of 360±180 pc. Without further observations it is difficult to definitively remove highly reddened M-dwarfs, however their contribution should not grossly affect our main goal.

5. DISCUSSION

Using a suite of Monte Carlo simulations and 15 HST/ACS parallel fields, we find a vertical scale height of 350±50 pc for the L- & T-dwarf population based on 28 faint candidates. This estimated scale height is consistent with the known trend of increasing scale height with decreasing stellar mass, independent of reddening, color selections, and other Galactic parameters and is within the uncertainties of and is largely a refinement of previous work (Liu et al. 2002; Pirzkal et al. 2005). Using our value of the scale height, and the parameters given in § 3, we predict a total of $\sim 10^{11}$ L- & T-dwarfs and a total mass of $\lesssim 10^{9}$ $M_{\odot}$ in the Milky Way.

This improved understanding of the L- & T-dwarf Galactic distribution will aide high-redshift surveys in better estimating the contamination of L- & T-dwarfs in their samples. In the recent HUDF pointed at $(\alpha,\delta)=(3^{\rm h}32^{\rm m}39^{\rm s}.0,-27^{\circ}47'29''.1)$ and a depth of $z'\sim 29$ mag, we predict $\gtrsim 2$ L- & T-dwarfs in its ~ 11 arcmin^{2} field of view, which has been confirmed by Pirzkal et al. (2005) who have spectroscopically identified three L- & T-dwarfs. We confirm that Galactic L- & T-dwarfs cannot significantly corrupt the $z\simeq 6$ surveys in high-latitude fields (the HUDF for example), however low-latitude fields will find a modest number of interloping L- & T-dwarfs. With only 28 candidates from 15 fields, our statistics remain sparse and ideally require further observations.

This work was funded by the ASU NASA Space Grant. The authors thank Dave Burstein and Neill Reid for their helpful discussions on Galactic structure and L- & T-dwarfs. The authors are greatly appreciative for the referee's insightful and useful comments. We wish to dedicate this work to the memory of Dr. John Bahcall.

Facilities: HST(ACS)

REFERENCES

Bahcall, J. N. 1986, ARA&A, 24, 577
Bahcall, J. N. & Soneira, R. M. 1980, ApJS, 44, 73
Bahcall, J. N. & Soneira, R. M. 1981, ApJ, 246, 122
Bahcall, J. N. & Soneira, R. M. 1984, ApJS, 55, 67
Bertin, E. & Arnouts, S. 1996, A&AS, 117, 393
Burgasser, A., Kirkpatrick, D., Burrows, A., Liebert, J., Reid. N., Gizis, J., McGovern, M., & Prato, L. 2003, ApJ, 592, 1186
Burgasser, A. J., et al. 1999, ApJ, 522, L65
Chabrier, G. 2001, ApJ, 554, 1274
Chabrier, G. 2002, ApJ, 567, 304
Cruz, K. C., Reid, I. N., Liebert, J., Kirkpatrik, J. D., Lowrance, P. J. 2003, AJ, 126, 2421
de Grijs, R., Peletier, R., & van der Kruit, P. 1997, A&A, 327, 966
Delfosse, X., Tinney, C. G., Forveille, T., Epchtein, N., Borsenberger, J., Fouqué, P., Kimeswenger, S., & Tipène, D. 1999, A&AS, 135, 41
De Marchi, G. et al. 2004, Detector Quantum Efficiency and Photometric Zero Points of the ACS, Instrument Science Report, (STScI, Baltimore)
Gilmore, G. 1984, MNRAS, 207, 223
Gilmore, G & Reid, N. 1983, MNRAS, 202, 1025
Gilmore, G., Wyse, R., & Kuijken, K. 1989, ARA&A, 27, 555
Hawley, S. et al. 2002,ApJ, 123, 3409
Herschel W. 1785, RSPT, 75, 213
Kapteyn, J. C. 1922, ApJ, 55, 302
Kirkpatrick, J. D., et al. 1999, ApJ, 519, 802
Kirkpatrick, J. D. 2000, AJ, 120, 447
Koekemoer, A. M., Fruchter, A. S., Hook, R., & Hack, W. 2002 "*The 2002 HST Calibration Workshop*" Space Telescope Science Institute, 2002
Larsen, J. A. & Humphreys, R. M. 2003, AJ, 125,1958
Liu, M., Wainscoat, R., Martín, E. L., Barris, B., & Tonry, J. 2002, ApJ, 568, L107
Majewski, S. R. 1993, ARA&A, 31, 575
Nakajima, T., Oppenheimer, B. R., Kulkarni, S. R., Golimowski, D. A., Matthews, K., & Durrance, S. T. 1995, Nature, 378, 463
Oke, J. B. & Gunn, J. E. 1983, ApJ, 266,713
Oppenheimer, B. R., Kulkarni, S. R., Matthews, K., & Nakajima, T. 1995, Science, 270, 1478
Porcel, C., Garzón, F., Jimenénez-Vicente, J., & Battaner, E. 1998, A&A, 330, 136
Pirzkal N., et al. 2005, ApJ, 622, 319
Reid, I. N. & Majewski, S. R. 1993, ApJ, 409, 635
Reid, I. N. 2003, AJ, 126, 2449
Reid, I. N., et al. 1999, ApJ, 521, 613
Robin, A., Reylé, C., & Crézé M. 2000, A&A 359, 103
Robin, A., Reylé, C., Derrière, S., & Picaud, S. 2003, A&A, 409, 523
Schlegel, D. J., Finkbeiner, D. P., & Davis, M. 1998, AJ, 500, 525
Siegel, M. H., Majewski, S. R., Reid, I. N., & Thompson, I. B. 2002, ApJ, 578, 151
Strauss, M. A., et al. 1999, ApJ, 522, L61
Tsvetanov, Z. I., et al. 2000, ApJ, 531, L61
von Seeliger, H. 1898, Abh. Bayerische Akad. Wiss., Math.-Phys. KI, 19, 564
Yan, H. & Windhorst, R. A. 2004a, ApJ, 600, L1
Yan, H. & Windhorst, R. A. 2004b, ApJ, 612, L93
Yan, H., Windhorst, R. A., & Cohen S. H. 2003, ApJ, 585, L93
Yan, H. et al. 2002, ApJ, 580, 725
Yamagata, T., & Yoshii, Y. 1992, AJ, 103, 117